6-15-2021

Impact of Green and White Roofs on Air Handler Filters and Indoor Ventilation Air

Pradeep Ramasubramanian
Portland State University, pradeep2@pdx.edu

Irvan Luhung
Singapore Center for Environmental Life Sciences Engineering (SCELSE)

Serene B. Y. Lim
Singapore Center for Environmental Life Sciences Engineering (SCELSE)

Stephan C. Schuster
Singapore Center for Environmental Life Sciences Engineering (SCELSE)

Olyssa Starry
Portland State University, ostarry@pdx.edu

See next page for additional authors

Impact of green and white roofs on air handler filters and indoor ventilation air

Pradeep Ramasubramanian

Portland State University, 1825 SW Broadway, Portland, OR 97201

Irvan Luhung

Singapore Center for Environmental Life Sciences Engineering (SCELSE), 60 Nanyang Drive, SBS-01N-27, Singapore 637551

Serene B.Y. Lim

Singapore Center for Environmental Life Sciences Engineering (SCELSE), 60 Nanyang Drive, SBS-01N-27, Singapore 637551

Stephan C. Schuster

Singapore Center for Environmental Life Sciences Engineering (SCELSE), 60 Nanyang Drive, SBS-01N-27, Singapore 637551

Olyssa Starry

Portland State University, 1825 SW Broadway, Portland, OR 97201

Elliott T. Gall

Portland State University, 1825 SW Broadway, Portland, OR 97201

*Corresponding author: Elliott T. Gall, gall@pdx.edu

Abstract

Rooftop surfaces near building outdoor air intakes may contribute to the mass loading on filters and compounds emitted to ventilation air downstream of the filter. In laboratory analyses, we characterized microbial composition, primary volatile organic compound (VOC) emissions, ozone removal rates, and VOC emissions in the presence of ozone on filters collected from air handlers located on the green and white roof sections of a big-box retail store. Total DNA masses per area of filter were 26.3 ± 11.9 ng cm^{-2} and 6.3 ± 6.5 ng cm^{-2} for green and white roof filters respectively, with higher mass observed in winter compared to the fall season. Of eight VOCs quantified at constant 23 ◦C and 50% RH across both seasons, fluxes of m/z 33.02 (putatively attributed to methanol) dominated VOC emissions for green, 10.96 ± 3.09 μmol m^{-2} hr^{-1}, white, 12.02 ± 3.41 μmol m^{-2} hr^{-1}, and unused filters, 5.64 ± 1.08 μmol m^{-2} hr^{-1}. Ozone removal across all filters varied from 3.5 % ± 2.8 % to 14 % ± 2.8%, depending on temperature and RH condition. Fluxes of eight quantified VOCs were lower in the presence of ozone, apart from m/z 69.07 (putatively attributed to isoprene), where the presence of ~180 ppb inlet ozone resulted in increased fluxes by a factor of ~2.4. A steady-state mass balance predicted increases in ventilation air methanol levels by green roof filters ranging 0.10 μg m^{-3} to 19.44 μg m^{-3}, depending on filter face velocity and filter geometry.

Keywords

HVAC filter, filter microbial composition, ozone removal, VOC fluxes, seasonal dependence

1. Introduction

Green roof implementation has been incentivized in many cities for their purported environmental, social and economic benefits such as storm-water management, building energy savings and reducing urban heat island effect[1–5]. Benefits to urban outdoor air quality from greenery and green roofs are also claimed,[6] but recent studies suggest impacts may be modest[7–9]. One explored avenue by which green roofs may affect exposure to air pollution is by altering indoor air quality. For example, as outdoor air is transported across green roof surfaces, particles from the substrate and vegetation may suspend and be entrained in the local rooftop air flow. Since outdoor air intake for buildings is frequently sited on rooftops, the particle-laden rooftop air flow may trap green roof particles onto rooftop filtration systems. A relatively unexplored connection between green roofs and air pollution exposure is via heating, ventilation, and air conditioning (HVAC) filters that process outdoor ventilation air entering from a green roof.

Loading of biotic matter on HVAC filters may alter the air quality of outdoor air ventilation.[10] For example, HVAC filters can be sources of indoor particles which can be composed of whole or fragmented abiotic and biotic matter[11]. Loaded filters can also contain microbes that can impact indoor air through the release of fungal spores from filters[12] due to turbulence and other microbial discharge mechanisms. The presence of microbes is mediated by environmental conditions; over a 14 day period of high relative humidity (RH), Möritz et al.[12] show microbes from filters enter the indoor environment; and to prevent fungal growth on filters, control of both temperature and RH were required[13].

Loaded filters can act as a source of volatile organic compounds (VOCs) to the indoor environment. A field study of secondary air filters in a multi-story office building found indoor VOCs related to fungal metabolic processes, and traced the source to fungal loading of filters[14]. As filter operational times increase, particle loadings increase which results in increased surface area for sorption/desorption processes[15]. Compounds such as carboxylic acids, aldehydes, terpenes and nitrogen-containing organic compounds are shown to be released from dust accumulated on filters[16,17]. Higher concentrations of formaldehyde,

68 acetaldehyde and acetone were found in loaded filters compared to unused filters, with acetone
69 concentrations increasing as filters becomes increasingly loaded[18].

70 As filter loading increases with run-time, filters remove greater quantities of ozone (O_3)[19], a common
71 urban air pollutant. Prior work has characterized ozone removal to loaded HVAC filters from office
72 spaces[20], residential and commercial filters[21], dusty and sooty filters[22], and to green roof and white roof
73 filters[10]. Ozone removal via the Criegee mechanism leads to carbonyl formation;[23] a linear correlation can
74 be made for carbonyl generation and ozone removal, when normalized for organic carbon mass on filters[24].
75 Ozonolysis products, including formaldehyde, acetaldehyde, acetone, and 4-oxopentanal are elevated
76 downstream of filters laden with particles from vegetation and diesel emissions[25]. Some products, including
77 formaldehyde, are emitted in proportion to RH level.[26] Different plant species variably produce isoprene[27]
78 and terpenes,[28] organic compounds that are reactive with ozone. If these reactive organics are present on
79 HVAC filters, surface reactions with ozone can lead to the formation of secondary organic aerosols[29–31]

80 In this manuscript, we examine the impact of loaded filters collected from a rooftop with vegetated
81 (green roof) and non-vegetated (white roof) areas to investigate the effect of surrounding rooftop type on
82 filter loading and the ensuing impact on VOC and particle emissions from filters. We characterize the
83 microbial loadings on filters as well as identify the emissions of VOCs in the absence of ozone (primary
84 VOC emissions), ozone removal rates, and emissions in the presence of ozone in a laboratory chamber
85 apparatus. These analyses are conducted for filters collected from the field site during the fall and winter
86 season. Despite the growing body of evidence linking HVAC filter quality to indoor air, to our knowledge,
87 this is the first study to explore microbial composition on filters, characterize the VOC fluxes in the absence
88 and presence of ozone, and report ozone removal rates for filters across various temperature and RH
89 conditions and multiple seasons.

90 ## 2. Material and Methods

91 ### 2.1. Field Site

92 The field site is in north Portland, OR, USA at the roof of a big-box retail store. The rooftop is
93 comprised of three extensive green roof sections varying according to substrate depth, (~3600 m^2 of total
94 green roof area) and a 'white' roof section (~5400 m^2) covered only in white waterproof membrane totaling
95 a combined rooftop area of 9,000 m^2 and shown in **figure S1**. The green roof design varies somewhat by
96 section but is generally comprised of a scoria-dominated substrate over a capillary fabric and waterproofing
97 membrane. The plant community is a mixture of succulent and herbaceous plants that were both planted
98 and introduced; dominant species include *Erodium cicutarium*, *Plectritis congesta*, *Phedmus*
99 *takesimensis*, *Sedum rupestre* 'Angelina', *Trifolium repens, and Vulpia sp.* As much as 20% of the roof
100 coverage was classified as rock/gravel. The field site is surrounded by urban surfaces to the south, vegetated
101 surfaces and urban greenery to the north and a major interstate highway (I-5) roughly ~1000 m to the west
102 of the field site. Air handling units (AHU) from which filters were taken were chosen based on their
103 location, as close to the center of each rooftop type as possible. The filters collected were outdoor ventilation
104 air filters only; the duty cycle of the outdoor air ventilation fans was unknown during the filter operational
105 period.

106 2.2. Filter Collection

107 Loaded filters (described as "green" and "white" roof filters hereafter) were collected from AHUs after
108 operation for three-month periods occurring from October 2018 – January 2019 (Fall season) and January
109 2019 – March 2019 (Winter season). Samples of filters (area of 17.35 cm^2) for analysis were randomly cut
110 from an intact filter, using sterilized stainless-steel scissors, from a filter taken from the AHU filter bank.
111 An unused filter of the same make (AAF PerfectPleat, HC M8) was acquired from maintenance personnel
112 immediately after the filter collection period. Filters were immediately sealed and stored in a polyethylene
113 bag at -15˚ C freezer until tested for DNA composition, ozone removal and VOC emissions.

114 2.3. Filter microbial composition analysis

The collected HVAC filter samples were cut inside a biological safety cabinet into 10 cm^2 pieces (5 x 2 cm) before being put into individual 5 mL tubes for biomass removal. For each filter panel, six random 10 cm^2 pieces from different parts of the panel were cut and analyzed for replication purposes. Biomass is first removed from the filter by washing with 6 mL phosphate buffer saline (PBS) + 0.1% v/v Triton X-100 (non-ionic detergent). The wash buffer containing the biomass is subsequently concentrated on 0.02 µm Anodisc (Whatman) using a vacuum manifold (DHI) and immediately subjected to DNA extraction. DNA was extracted with Qiagen DNeasy Power Water kit following the manufacturer's protocol with slight modifications to improve DNA yield. Briefly, during cell lysis step, a 30-min 65°C water bath incubation was added before the recommended 5-min bead-beating step[32].

After extraction, total DNA concentration was quantified using Qubit 2.0 fluorometer with dsDNA HS (high sensitivity) kit (Invitrogen) and finally presented in ng of DNA per cm^2 of filter. Concurrently, Metagenomic sequencing was also performed on the extracted DNA samples with shotgun approach. Accel-NGS 2S Plus DNA kit (Swift Biosciences) was used to create the sequencing libraries. DNA was first sheared with Covaris S220 or E220 focused ultra-sonicator to 450bp size. Dual-barcodes with indices from the 2S Dual indexing kit (Swift Biosciences) were then added to all libraries and validated on the Bioanalyzer DNA 7500 chip (Agilent). Finally, library concentrations were normalized to 4 nM and pooled at equal volume for sequencing on Illumina HiSeq 2500 platform with rapid runs at a final concentration of 10-11 pM and read length of 251 bp paired ends (Illumina HiSeq 2500 V2 rapid sequencing chemistry).

The resulting raw sequences were first subjected to adapter removal and quality trimming (Phred quality Q20) with Cutadapt v 1.8.1[33]. Trimmed reads were then aligned to NCBI non-redudant (nr) protein database (ver. 22 November 2019) with a maximum of 5 allowed mismatches and e-value cutoff of 0.01 for taxonomic assignment with Kaiju[34]. The outputs were finally visualized with MEGAN v6.17[35] and the final DNA composition of the filter samples was presented in percentage (%) of assigned reads at phylum level. All raw sequences used in this study have been uploaded to the National Center for Biotechnology Information (NCBI) Sequence read archives (SRA) under bioproject accession number PRJNA681296.

2.4. Filter chamber-oxidation analysis

Filters were tested for emissions of VOCs in the presence and absence of ozone and ozone removal in the apparatus shown in **figure 1.** The apparatus uses filtered and humidified compressed air that is injected into a temperature-controlled filter cartridge assembly for VOC emissions and ozone removal measurement.

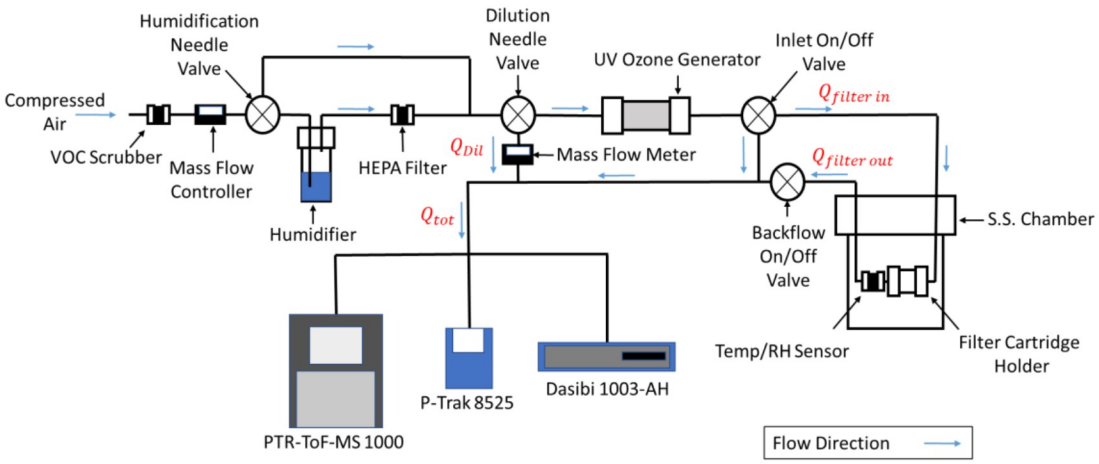

Figure 1. Filter chamber set up for primary emissions, ozone deposition and emissions in the presence of ozone.

The apparatus uses an activated carbon filter (IRAC40, Ingersoll-Rand, Ireland) prior to humidification and a HEPA filter (HC01U-4N-B, ETA Filters, USA) after the humidifier, the latter necessary as we observed an elevated background particle number due to the humidification. Humidification is regulated using a 1000 mL gas-washing cylinder (LG-3765-130, Wilmad Lab Glass, USA) filled with distilled water and a needle valve to control the flow into the humidification cylinder. Ozone generation is controlled using a shortwave (185 nm) UV photochemical ozone generator (SOG-1, AnalytikJena, Germany). A dilution flow is used to provide adequate flow to the instruments, 2 LPM, while maintaining a filter face velocity of 1.1-1.3 cm s^{-1}, chosen for consistency with prior bench-scale laboratory analysis[10,36]. Filters are placed in a PFA filter holder (PFA 225-1712, Savilex, USA) inside a temperature controlled stainless steel chamber. A 12-Bit combined temperature and relative humidity (RH) sensor (S-THB-M008, Onset, USA) is used to measure the temperature and RH of the air. Ozone is measured using a UV ozone analyzer (1003-AH,

158 Dasibi, USA). Particle counts (0.02 – 1 μm) are measured using through a P-Trak Ultrafine Particle Counter
159 (P-Trak Ultrafine Particle Counter 8525, TSI, USA).

160 Primary VOC emissions and VOC emissions in the presence of ozone were measured using a proton
161 transfer reaction – time of flight – mass spectrometry (PTR-TOF-MS 1000, Ionicon, Austria) with H_3O^+ as
162 the primary reagent ion (O_2^+ and NO^+ signal intensities were respectively less than 5% and 1% of $H_3{}^{18}O^+$
163 and water cluster ($(H_2O)H_3O^+$) intensities around 1-2% of $H_3{}^{18}O^+$). Drift tube conditions were T_{drift} = 60°C,
164 P_{drift} = 2.20 mbar, U_{drift} = 600 V, which resulted in electric field strength to number density ratio E/N = 135
165 Td (Townsend, 1 Td = 10-17 V cm^2). The mass axis calibration was performed using three peaks: NO^+ (m/z
166 = 29.9974), $C_3H_7O^+$ (m/z = 59.0497) and a $C_6H_4I_2$ fragment (m/z = 203.944) via an internal standard
167 continuously injected into the drift tube via a heated permeation device (PerMaScal, Ionicon Analytik
168 GmbH, Innsbruck, Austria). Mass spectra were stored in 30 s intervals. The inlet was held at 60°C and the
169 supplemental inlet flow to the drift tube was set at 150 mL min^{-1}.

170 A peak list of compounds of interest was chosen based on the potential for emissions from biotic matter
171 and precursors for byproduct formation and oxidation byproducts[37–46]. These compounds are shown in **table**
172 **S1** of the supporting information document. Putative IDs of these compounds are: methanol (m/z 33.03),
173 acetaldehyde (m/z 45.03), formic acid (m/z 47.01), acetone (m/z 59.04), acetic acid (m/z 61.03), isoprene
174 (m/z 69.07), and monoterpenes (m/z 137.12).

175 2.5. Experimental protocol

176 Loaded and unused field filter samples were cut to flat circular samples of diameter of 47 mm and
177 placed in the filter holder. The filter sample is compressed between two mating PFA surfaces and the
178 operative area exposed to airflow (ozone free or containing ozone) was 17.35 cm^2. Prior to each experiment,
179 the filter cartridge is cleaned and passivated at 200 ppb ozone for 12 hours to remove any confounders due
180 to cartridge handling. Three relative humidity and three temperature conditions were tested for the fall
181 season filters: 20%, 50% and 80% RH and 15 °C, 23 °C and 31 °C, respectively. Temperatures were chosen

to characterize the behavior of filters across realistic outdoor temperatures. The range was selected to span >10 ◦C, as a rule of thumb (Arrhenius equation) predicts will lead to a doubling of the reaction rate, while considering limitations of our laboratory setup to maintain elevated and lowered chamber concentrations for the duration of each experiment. High and low temperature and RH conditions were tested in duplicates for the fall season. The median condition, 50% RH and 23 °C, was tested in triplicates for the fall and winter season. A flow rate of 1.2-1.4 L min^{-1} of air is sent to the filter cartridge, resulting in a face velocity of 1.1-1.3 cm s^{-1}. Measurements were split into two 2.5 h segments for each filter; the first segment was to measure filter primary VOC emissions and downstream particle concentration and a second segment to measure filter ozone removal efficiencies, secondary organic aerosol formation and VOC emissions in the presence of ozone. For each 2.5 h segment the inlet concentration was measured for the first 0.5 h, the outlet concentration measured for the next 1.5 h and finally the inlet concentration was measured again for 0.5 h (**figure S2)**. For the first 2.5 h segment, O_3 levels were <2 ppb and during the second segment ozone was injected, with filter holder inlet levels ranging 170-190 ppb. Experiments were run in duplicate, except for the median temperature and RH conditions (23 °C and 50% RH) for the fall and winter data set, which was run in triplicate. The averaged concentrations reported here are the time-average of the final 30 minutes of the 1.5 h outlet measurement. This period met the steady-state conditions for ozone, <2 ppb change over 10 mins[47].

3. Theory/Calculation

3.1.1. Volatile organic source and sink strength quantification

Primary VOCs were calculated according to the following equation:

$$\overline{F_{filter}} = \left[\left[\left(\frac{\overline{C_{i,tot_{out}}} \times Q_{tot_{out}} - \overline{C_{i,in}} \times Q_{dil_{out}}}{Q_{filter\,out}} - \overline{C_{i,in}}\right) \times \frac{Q_{filter\,out}}{A}\right] \times \alpha\right] - \overline{F_{background}} \quad [1]$$

where subscripts 'out' and 'in' represent the flow through the filter chamber and flow bypassing the filter chamber, respectively. The mean primary VOC flux from the filter (μmol m^{-2} h^{-1}) is $\overline{F_{filter}}$, $\overline{C_{i,tot_{out}}}$ is the

mean total outlet concentration of compound i (ppb), $Q_{tot_{out}}$ is the total flow during the respective outlet period (L min^{-1}), $\overline{C_{i,in}}$ is the mean inlet concentration of compound i (ppb), $Q_{dil_{out}}$ is the dilution flow during the outlet measurement period (L min^{-1}), $Q_{filter\ out}$ is the flow measurement at the outlet of the filter (L min^{-1}), A is the area of the exposed filter (m^2), α is the unit conversion factor to convert from units of ppb L m^{-2} min^{-1} to units of μmol m^{-2} h^{-1} and depends on the molecular weight of the specific compound, and finally $\overline{F_{background}}$ is the mean background VOC flux (μmol m^{-2} h^{-1}) in the absence of a filter. Time-averages for $\overline{C_{i,\ tot_{out}}}$ and $\overline{C_{i,in}}$ were taken over the last 30 minutes of the oulet and inlet period, respectively. $Q_{filter\ out}$ was calculated by subtracting $Q_{dil_{out}}$ from $Q_{tot_{out}}$.

VOC emissions in the presence of ozone was calculated in a similar manner and shown below:

$$\overline{F_{filter_{O3}}} = \left[\left[\left(\frac{\overline{C_{i,\ tot_{out}}}\times Q_{tot_{out}} - \overline{C_{i,\ in_{0ppb}}}\times Q_{dil_{out}}}{Q_{filter\ out}} - \frac{\overline{C_{i,\ tot_{in}}}\times Q_{tot_{in}} - \overline{C_{i,\ in_{0ppb}}}\times Q_{dil_{in}}}{Q_{filter\ in}}\right)\times\frac{Q_{filter\ out}}{A}\right]\times\alpha\right] - \overline{F_{background}} \quad [2]$$

where the second part of the right side of the equation represents the potential change in concentration of compound i (ppb) with respect to the increased ozone concentration. $\overline{C_{i,\ in_{0ppb}}}$ is the mean inlet concentration of compound i at 0 ppb ozone (ppb), $\overline{C_{i,\ tot_{in}}}$ is the mean total inlet concentration of compound i (ppb), $Q_{tot_{in}}$ is the total flow during the inlet measurement period (L min^{-1}), $Q_{dil_{in}}$ is the dilution flow during the respective measurement period (LPM), and Q_{in} is the ozonated inlet flow (L min^{-1}). $Q_{filter\ in}$ was measured through bypassing the filter chamber and calculated by subtracting $Q_{dil_{in}}$ from $Q_{tot_{in}}$.

3.1.2. Ozone removal

The removal of ozone to filters was characterized using fractional removal efficiency provided by

$$\eta = 1 - \frac{\frac{C_{i,\,tot_{out}} \times Q_{tot_{out}}}{Q_{filter\ out}}}{\frac{C_{i,\,tot_{in}} \times Q_{tot_{in}}}{Q_{filter\ in}}} \quad [3]$$

where η is removal efficiency (%), $\overline{C_{i,\,tot_{out}}}$ and $\overline{C_{i,\,tot_{in}}}$ are the mean outlet and inlet ozone concentration in (ppb) and the other variables are previously mentioned. Averages for $\overline{C_{i,\,tot_{out}}}$ and $\overline{C_{i,\,tot_{in}}}$ were taken over the last 30 minutes of the respective experimental period.

3.1.3. Contribution to ventilation air

The contribution of filter emissions to ventilation air downstream of the filter is provided by a mass-balance on a volume of air passing through the air-handler containing a filter[25]:

$$C_{in} = C_{out} + \frac{F_{filter} \times R}{V \times \beta} \quad [4]$$

where C_{in} and C_{out} are inlet (μg m^{-3}) and outlet concentrations upstream and downstream a hypothetical filter, respectively, F_{filter} is the emission flux (μg m^{-2} h^{-1}) converted from units of μmol m^{-2} h^{-1}, R is the ratio of filter media surface area to filter face area (dimensionless), V (m s^{-1}) is the filter face velocity, and β is the unit conversion factor (3600 s h^{-1}). R values can vary depending on the type of filter; pad filter (R=1), pleated filter (R=4), thick pleated filter (R=10), and bag filter (R=19). The contribution of the filter to the indoor concentration is given by $\frac{E \times R}{V}$.

3.1.4. Statistical analysis and uncertainty propagation

Shapiro-Wilk tests were used to check normality of log-transformed fluxes of selected compounds across seasonal, temperature and RH datasets. Shapiro-Wilk tests with output p-value < 0.05 were ignored from ANOVA tests. A three-way ANOVA considered the effects of season (fall and winter), filter type (green and white), and trial (non-ozonated and ozonated) and associated interactions on compounds from the seasonal dataset that passed the Shapiro-Wilk tests, presented in **table S2**. Data on unused filters was not included in these analyses, as season is not an independent variable of unused filters. A three-way

unbalanced ANOVA was performed on temperature (15 °C, 23 °C and 31 °C), filter type (green, white and unused), and trial and their associated interactions on compounds that passed the Shapiro-Wilk tests for the temperature dataset and shown in **table S3**. A similar three-way unbalanced ANOVA considered the effects of RH (20%, 50% and 80% RH), filter type (green, white and unused), and trial and associated interactions on compounds that passed the Shapiro-Wilk tests for the RH dataset, presented in **table S4**. A Tukey multiple comparison post hoc test was employed for all three-way ANOVA tests.

A Friedman's test was applied, similar to a one-way ANOVA with repeated measures[48,49], for filter type (green, white and unused) across the two trial conditions (non-ozonated and ozonated) for the selected compounds that did not pass the Shapiro-Wilk normality tests for the fall season dataset, shown in **table S5**. A Dunn's pair wise post hoc analysis was performed between the ranks of the Friedman's test and a Bonferroni post hoc correction for multiple tests was applied. A p-value ≤ 0.05 was deemed a significant difference among the variables tested for each dataset. All statistical tests, analysis and graphs were performed and generated in MATLAB.

Uncertainty for VOC fluxes at each condition was estimated by propagating the difference between the maximum and minimum averaged concentrations across replicates for each selected compound. Propagated uncertainty for ozone removal was calculated using 2% instrumentation error on inlet and outlet concentrations.

4. Results and Discussion

An illustrative dataset collected from chamber studies is shown in **figure 2**, with green roof filter data shown for select VOCs, particle number concentrations, and inlet and outlet ozone levels at 23° C and 50% RH. Results from the experiments on fall filters studied across all temperature and RH conditions are presented in **table S6**. VOC fluxes were calculated based on **eq. 1 and eq. 2** and normalized to background concentrations. Periods in which the background concentration is higher is due to the filter behaving as a sink and shown as a negative flux in **table S6**.

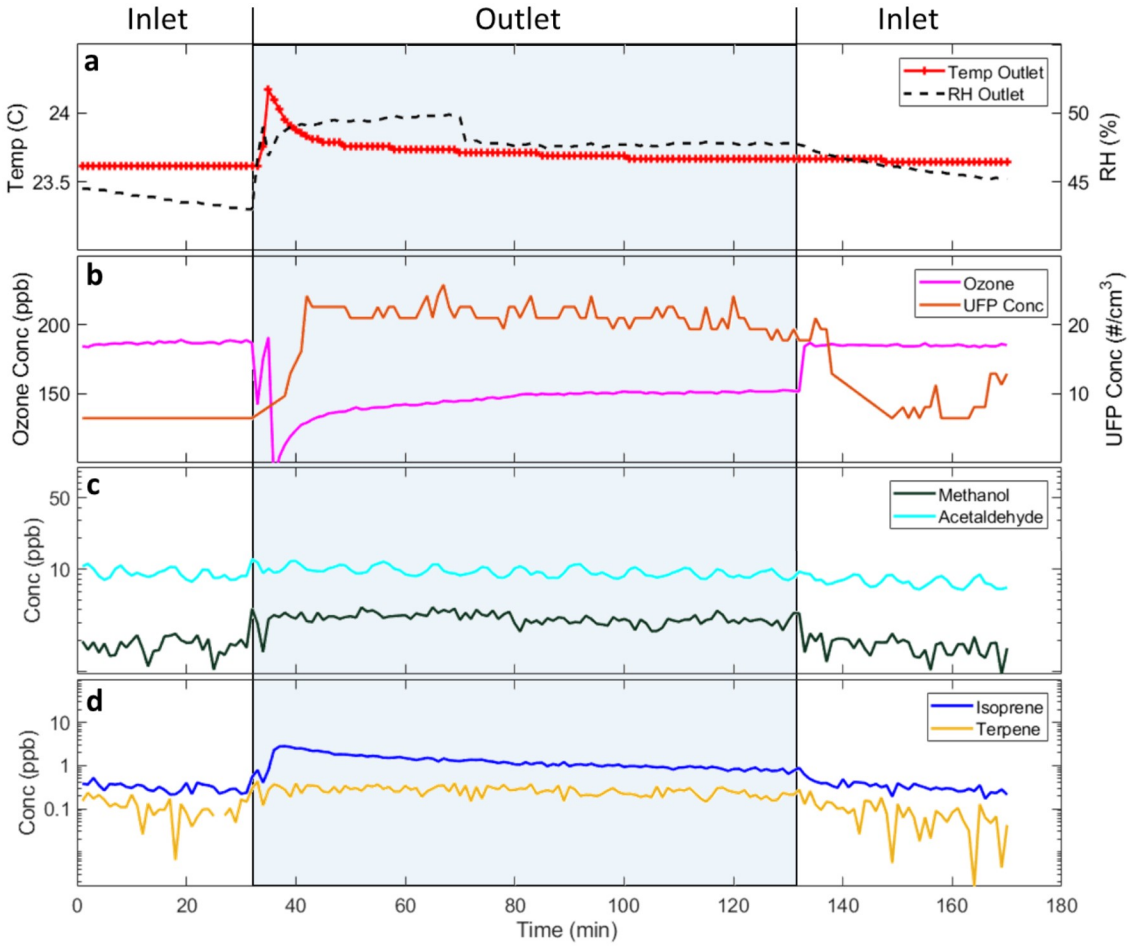

Figure 2. Representative measurements from filter ozonolysis experiment for fall season green roof sample at the 23° C and 50% RH. The inlet concentrations are measured in the first ~30 mins, then ~90 mins of outlet concentrations are measured (shaded area) and finally ~40 mins of inlet concentrations **a.** Temp (C) and RH (%) **b**. Ozone (ppb) and Particle number concentration ($\frac{\#}{cm^3}$) concentration **c.** Methanol (ppb) and Acetaldehyde (ppb) concentrations **d.** Isoprene (ppb) and Terpene (ppb)

4.1. VOC fluxes from green, white, and unused filters

Green and white roof filters were significantly more emissive than unused filters and methanol fluxes dominated the VOC fluxes that were tracked. Compounds of interest for this study were methanol (CH_3OH), acetaldehyde (C_2H_4O), formic acid (CH_2O_2), acetone (C_3H_6O), acetic acid (CH_3COOH), isoprene (C_5H_8) and terpenes ($(C_5H_8)_n$); emission fluxes are reported in full in **table S6** of supporting information. For the fall season at 23° C and 50% RH, methanol emissions from green and white filters are

similar in magnitude at 10.96 ± 3.09 and 12.02 ± 3.41 μmol m^{-2} hr^{-1}, respectively, and were significantly more emissive than the unused filters which measured 5.64 ± 1.08 μmol m^{-2} hr^{-1}. Methanol fraction of the total flux of the selected compounds were between 60-100% for green and white filters after background (empty filter holder) emissions were accounted for. Methanol fluxes from filters may be partially a result of cellulose composition of filters[18]. Cellulose composes many plant and wood walls[50,51] and methanol has been found to be a major component of VOC fluxes from plant and wood material[52], potentially explaining the high methanol flux in unused filters. Higher fluxes of methanol from green and white roof filters could be due to numerous reasons, including; local plant leaf emissions of methanol being sorbed and desorbed from filters[40], suspension and entrapment of soil or plant litter, which can include cellulose containing biotic matter, leading to emissions of methanol[53,54], or anthropogenic sources such as traffic that could emit methanol that is sorbed onto HVAC filters[55].

Primary fluxes of isoprene and terpenes, which are known precursors for secondary organic aerosol formation, were small across all temperature, RH, and seasonal conditions; 0.07 ± 0.08 and 0.01 ± 0.08 μmol m^{-2} hr^{-1} respectively, relative to other compounds for all filter types. One possible explanation is that since the filters were stored for roughly four months in a polyethylene bag at -15° C freezer, active plant cells trapped on filters may have deteriorated and lost their ability to perform metabolic processes that produce isoprene and terpenes[56,57]. Another potential rationale for the low terpene flux may be due to these compounds being more strongly sorbed to the filter or dissolved in a reservoir where the mass transfer across the boundary of the reservoir is much slower[58].

Methanol fluxes were lower in the presence of ozone, suggesting methanol consumption during ozonolysis and potential for secondary biproducts. Furthermore, isoprene fluxes increased in the presence of ozone for green roof filters, increasing from 0.15 ± 0.41 to 0.40 ± 0.22 μmol m^{-2} hr^{-1}, and for white roof filters, from 0.17 ± 0.30 to 0.38 ± 0.33 μmol m^{-2} hr^{-1}. We speculate this may result from a few possibilities including; fragmentation of a compound that may lead to a signal at m/z 69.07 or breakdowns and responses of organic matter present on the filter due to oxidation processes that lead to increases in gas-phase isoprene

309 concentrations. Ozone is known to cause death amongst gram-positive and gram-negative bacteria[59] and is
310 suggested in the food industry as a disinfecting agent[60]. This bacterial destruction could introduce isoprene
311 in the gas-phase from responses in bacterial metabolic mechanisms[61–63]. Another possibility for isoprene
312 emissions in the presence of ozone could be due to plant cells trapped on loaded filters as some plants are
313 known to emit isoprene as a method of reducing oxidative damage to the plant[64]. Isoprene synthesis has
314 been shown to occur on transgenic tobacco plants to prevent oxidative damage[65] and leaves themselves
315 have been shown to emit isoprene and nitric oxide (NO) during oxidative stress as a protection mechanism[66].

316 4.2. Ozone Removal for green, white, and unused filters

317 Ozone removal across filters varied between 3.5 % ± 2.8 % to 14 % ± 2.8 % depending on the type of
318 filter, temperature, and RH condition, shown in **figure 3**. Overall, removal efficiencies were in the range of
319 those previously reported; Abbass et al.[10] found ozone removal efficiencies for green roof and standard
320 rooftop filters were 5 % ± 2.8 % to 14 % ± 2.8 % removal at 21° C across 30% and 70% RH with an inlet
321 ozone concentration of 120 ppb.

322 White and green filter removal efficiencies increased as a function of RH, while the unused filters did
323 not vary across RH (**figure 3a**). Similarly, unused filters did not vary across temperature conditions (**figure**
324 **3b**), maintaining approximately 7 % ± 2.8 % to 8 % ± 2.8 % removal across all changes in temperature.

325 Ozone removal to filters increased as a function of increasing RH, shown in **figure 3a**, but effects of
326 temperature (**figure 3b**) were within propagated uncertainty. The highest removal was detected at 80% RH
327 at 23° C, which compares well with prior work that reported ozone removal doubles when RH is increased
328 from 24% RH to 80% RH[67]. Removal of ozone to filters has been shown to decrease with time[20,22], but,
329 removal efficiencies have been shown to partially recover after filters were treated with clean, non-ozonated
330 air[20]. **Figure 3c** shows ozone removal efficiencies as a function of season and is discussed in further detail
331 in **section 4.4.2**.

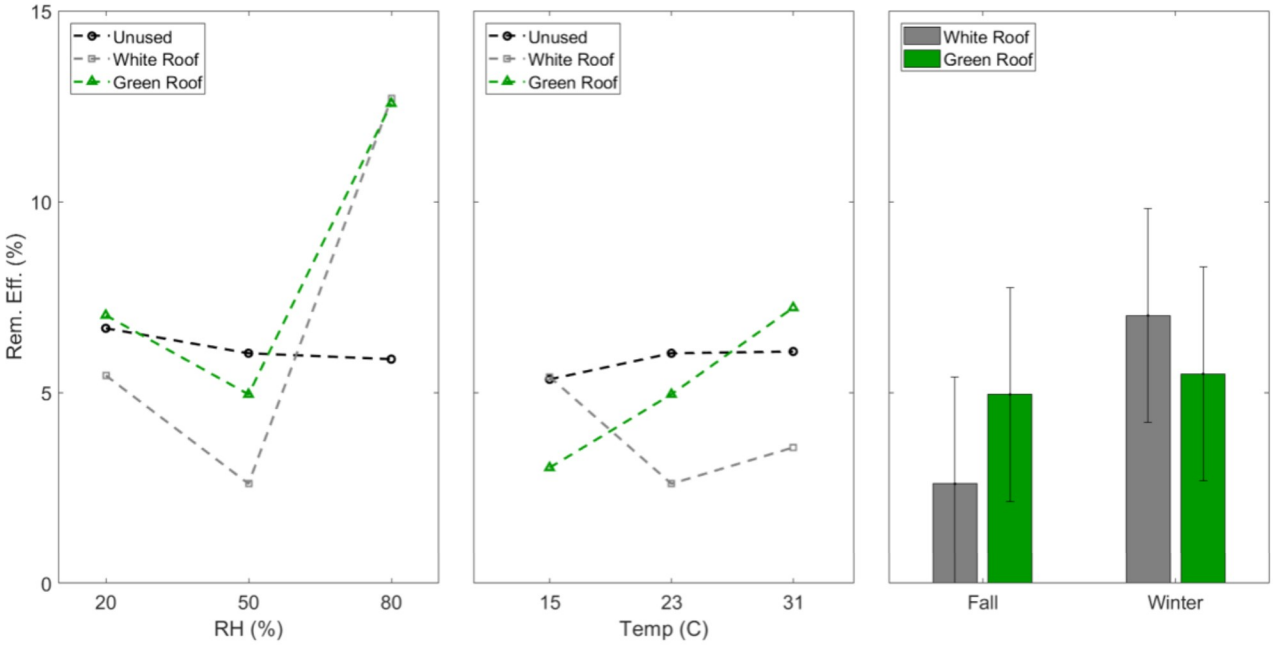

Figure 3. **a.** Ozone removal efficiency (%) for fall filters as a function of RH (%) **b.** Ozone removal efficiency (%) for fall filters as a function of Temp (C) **c.** Ozone removal efficiency (%) as a function of season (fall and winter). Unsused filters were ignored for the seasonal dataset as seasons have no impact to unused filters. Propagated instrumentation error was calculated to be ± 2.8 % removal efficiency for all tests.

4.3. Microbial characteristics of green and white roof filters

The microbial characterization of the HVAC filter samples is presented in **figure 4**. The green and white roof filters harbor distinct microbial contents in terms of both absolute and relative abundance. Green roof microbial communities change with plant community as well as environmental conditions[68], and this could explain some of the patterns in filter characteristics observed. The total DNA concentration extracted from the green roof samples was at least double the amount extracted from the white roof samples for both fall and winter samples (**figure 4a**). Differences in microbial composition between the two filter types are more apparent in winter as compared to fall season with DNA from plant taxa dominating the green roof filters (**figure 4b-d**). In the fall, both green and white filters were dominated by fungi, especially Ascomycota., which were also the most abundant phyla found in a study of green roof substrates in NYC[68]. In winter, green roof filters were characterized by plants from Streptophyta, and white roof filters were

characterized by Proteobacteria. Streptophyta encompasses some freshwater algae as well as bryophytes and mosses which are common winter active species found on green roofs in Portland[69]. As the filters only processed the ambient outdoor air, this finding reaffirmed how the roof types affected the amount and composition of particles depositing on the HVAC filters.

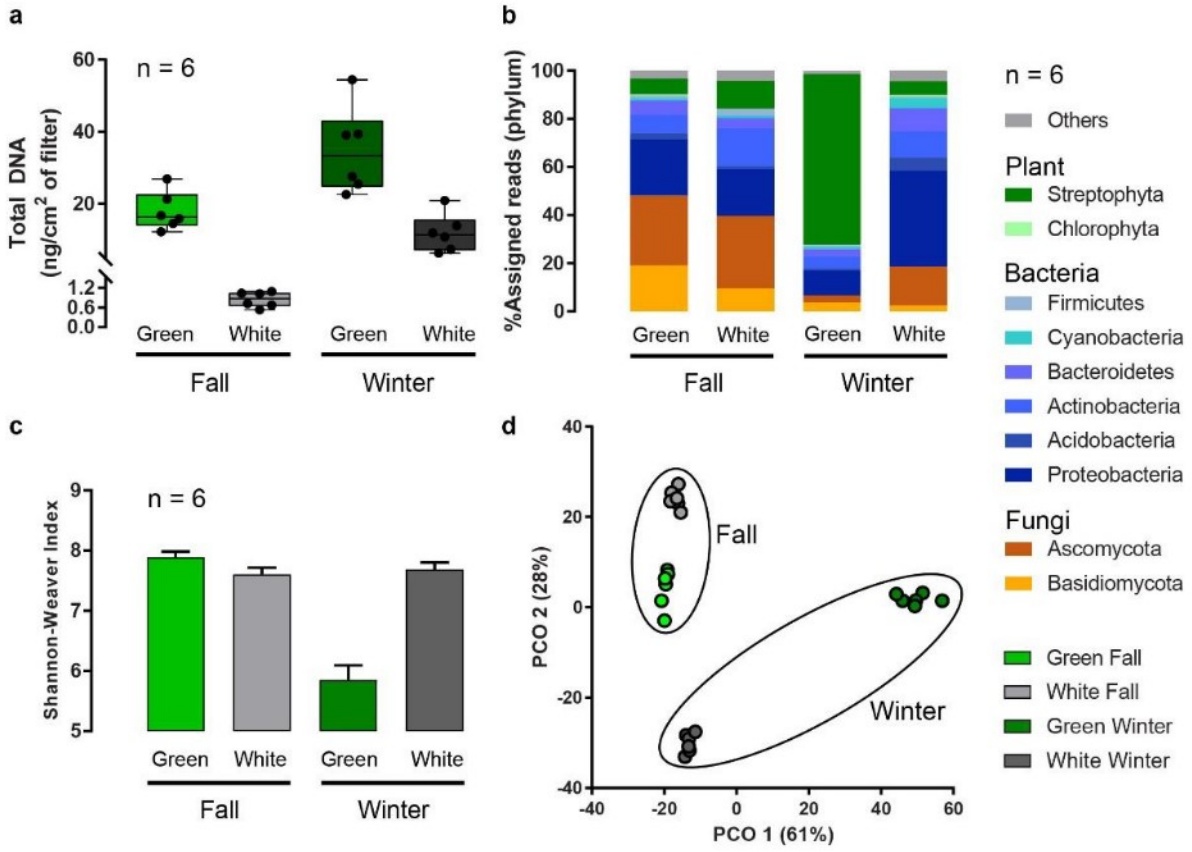

Figure 4. Microbial characteristics of the HVAC filters from green roof (green) and white roof (grey) buildings collected during fall (lighter shade) and winter (darker shade) **a.** Total DNA concentration per cm^2 area of filter **b.** Microbial composition in percentage of assigned reads on phylum level **c.** Shannon-Weaver diversity index **d.** Principal coordinates analysis (PCO) based on BrayCurtis similarity matrix**.** The error bars represent standard deviation with 6 replicates each per filter category.

4.4. Seasonal variation across green roof and white roof filters

4.4.1. VOC emissions across winter and fall seasons

Primary fluxes for selected compounds were higher in the fall relative to winter seasons. Primary fluxes of methanol at 23° C and 50% RH were higher for fall season filters, 11.49 ± 0.40 μmol m^{-2} hr^{-1}, compared to winter filters, 4.35 ± 0.85 μmol m^{-2} hr^{-1}, and shown in **figure 5a**. In comparison to the microbial analysis,

fall season had a greater fungal DNA fraction, and this difference may explain the higher methanol fluxes for the fall season filters as fungal degradation of plant cell walls have been shown to form methanol[70]. Primary fluxes of acetaldehyde, formic acid, acetone, and acetic acid were low in magnitude across both fall and winter periods.

Fluxes in the presence of ozone exhibited similar seasonal behavior as primary fluxes; higher fluxes of methanol for fall season filters, 3.99 ± 1.26 μmol m^{-2} hr^{-1} in relation to the winter filters, 1.74 ± 0.50 μmol m^{-2} hr^{-1}. Higher fluxes of acetaldehyde, an established byproduct of ozonolysis[71–74]; was also found in the fall season filters, 1.29 ± 0.94 μmol m^{-2} hr^{-1} versus winter filters, 1.08 ± 0.57 μmol m^{-2} hr^{-1}, shown in **figure 5b**. Formic acid, another byproduct of ozonolysis[71–74], had similar behavior however the differences were within propagated uncertainty. Higher fluxes of methanol and acetaldehyde were found on the fall season green roof sample compared to all other filter samples. Total VOC fluxes of the selected compounds were lower in the presence of ozone but increases in acetaldehyde and formic acid fluxes can have detrimental effects to human health and function[75,76]. There is also potential for increases in fluxes of compounds not tracked in this study.

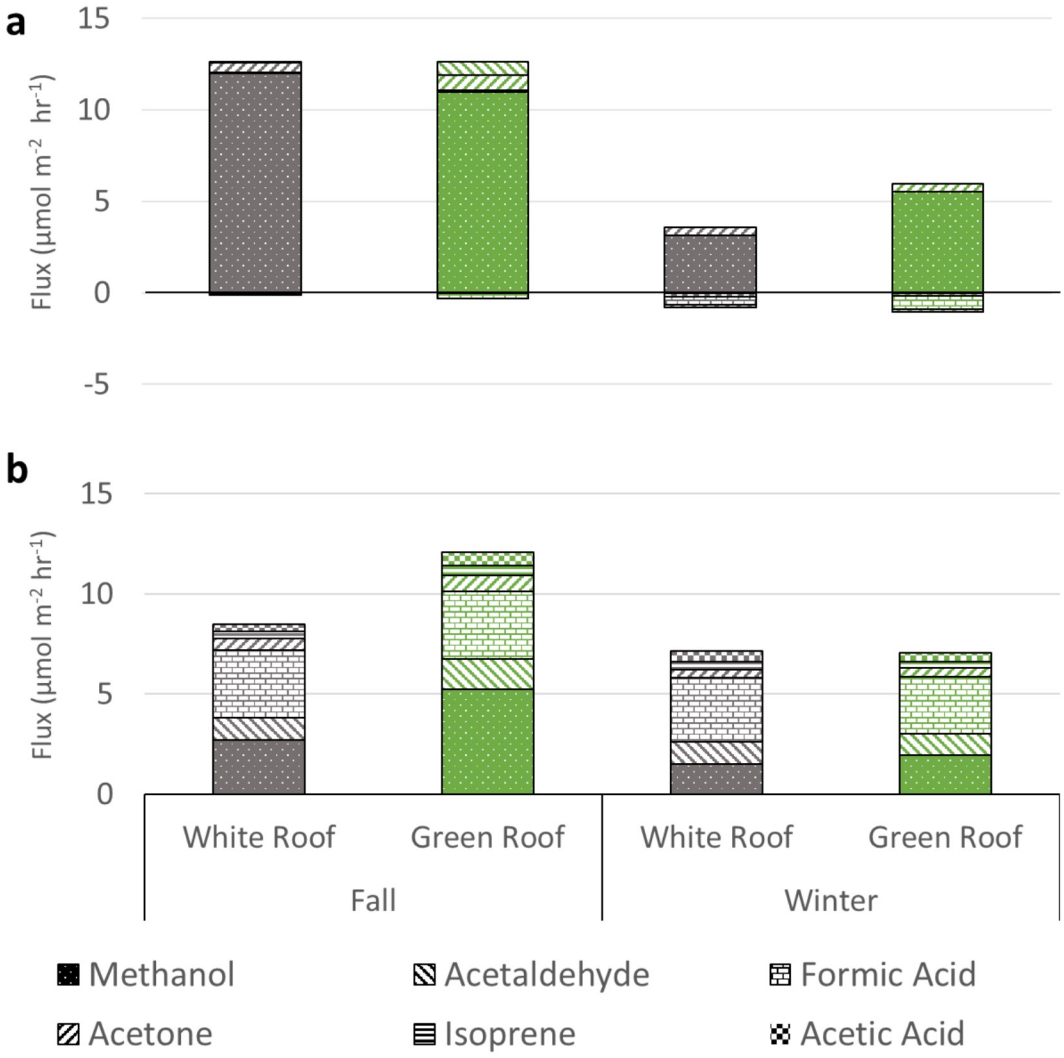

379

380 **Figure 5**. **a.** Averaged white roof and green roof primary VOC fluxes for selected compounds across
381 seasons at 23° C and 50% RH **b.** Averaged white roof and green roof VOC fluxes in the presence of
382 ozone for selected compounds across seasons at 23° C and 50% RH

383 4.4.2. Ozone removal across winter and fall seasons

384 Ozone removal for green roof and white roof filters were higher in the winter season, 6.5 % ± 2.8 %
385 and 8.0 % ± 2.8 % respectively, than those for the fall season, 5.9 % ± 2.8 % and 3.6 % ± 2.8 % respectively,
386 though the differences were within propagated uncertainty, shown in **figure 3c**. Green roof filters had
387 similar removal efficiency across the two seasons, but the differences again fell within propagated
388 uncertainty.

4.4.3. Microbial variation across winter and fall seasons

Across both fall and winters seasons, more biomass deposited on the green roof filters than the white roof filters. The DNA concentration difference was substantially higher in fall season (avg. 21-fold) compared to winter season (avg. 3-fold) (**figure 4a**). In contrast, the relative composition of the loaded matter on the filter were more distinct in winter season between the two roof types. The relative abundances of the top phyla (f**igure 4b**), the diversity index (**figure 4c**) and the PCO analysis (**figure 4d**) indicated that while the biomass compositions of the two roof types were similar in fall season, they were significantly different in winter. Taxa originated from plants dominated the green roof filters in winter. On average, the proportion of fungal taxa was higher during fall season than winter season for both types of filters. This result suggests that environmental conditions (e.g. temperature, RH) associated with different seasons also, directly or indirectly, impacted particle deposition on the HVAC filters.

4.5. VOC Fluxes due to changing temperature and RH conditions

Fluxes for the selected compounds varied highly between filter samples for each temperature and RH condition and shown in **table S2**. Temperature was not a statistically significant indicator of VOC fluxes of the selected compounds that passed the Shapiro-Wilks test criteria. RH was found to be a statistically significant indicator of filter fluxes of formic acid, acetone, and isoprene. Further statistical analysis on filter VOC fluxes as a function of temperature and RH could not be performed due to the non-normality of the dataset. The green roof filter generally had higher total VOC flux of the selected compounds, with the white roof having higher total VOC flux under high RH conditions.

4.6. Low SOA formation from oxidation processes on filters

The aerosol number formation (ANF) yield was calculated based on equation 4 present in Wang and Waring[29] and the average ANF amongst the green, white, and unused filters across all temperature and RH conditions was, $0.2 \pm 1.7 \frac{\#}{cm^3}/\frac{\mu g}{m^3}$, with the green roof sample at 23° C and 50 % RH being the highest at $0.64 \pm 1.2 \frac{\#}{cm^3}/\frac{\mu g}{m^3}$. For comparison, Waring and Seigel found ANF due to surface reactions and gas phase

413 reactions with d-Limonene was 126-339 $\frac{\#}{cm^3}/\frac{\mu g}{m^3}$ and 51.1-60.2 $\frac{\#}{cm^3}/\frac{\mu g}{m^3}$ [30] and Wang and Waring found
414 ANF varied around 2 $\frac{\#}{cm^3}/\frac{\mu g}{m^3}$ for ozone reactions with surface-sorbed squalene[29]. Low aerosol number
415 fractions are expected given observation of low concentrations of reactive organics (isoprene and
416 monoterpenes) emitted from filters; we speculate that this implies there exist low concentrations of surface-
417 sorbed monoterpenes on tested filter. For comparison, Waring and Seigel, in a study of the role of surfaces
418 to impact SOA formation from oxidation of d-limonene performed experiments with gas-phase
419 concentrations between 400 and 600 ppb,[30] whereas average concentrations of monoterpenes downstream
420 loaded and unloaded filter samples varied between 0.2 and 1 ppb in this study.

421 A thorough study of filter surface properties was not conducted but may be warranted to better
422 understand the fundamental roles of the surface sorbed compounds to the gas-phase filter emissions. Surface
423 environmental scanning electron microscope (ESEM) images and solvent extraction methods are potential
424 ways to better understand the surface properties[10,77] and chemical composition of filter loaded mass, lending
425 further mechanistic insight into what conditions may yield secondary aerosol formation from surface
426 ozonolysis of filters. Future studies could also consider testing filters in-situ, e.g., by generating ozone on-
427 site or immediately after sampling from the field; it is possible that volatile reactive organics were lost in
428 our sample handling and storage.

429 4.7. VOC contribution to the indoor environment

430 Results of the estimate of the impact of primary emission of VOCs from filters on ventilation air quality
431 (i.e., air downstream a hypothetical filter, emitting at rate measured in this study) is made using **equation**
432 **4**. A median face velocity, 0.5 m s^{-1} was chosen to represent typical flow rates for a 1 m^2 filter area[25], and
433 a high and low value of 1 m s^{-1} and 0.1 m s^{-1} was chosen to represent high and low HVAC air flow conditions
434 respectively. Low face velocities are on the order of 360 m^3 h^{-1}/(m^2 filter area) and high face velocities are
435 approximately 3600 m^3 h^{-1}/(m^2 filter area). Steady-state contribution to indoor ventilation air for five VOCs
436 for green and white roof filters at various face velocities and 'R' values are given in **table S7.**

Steady state increase in methanol concentration in ventilation air for various filter pleats under different face velocities is shown in **figure 6**. For loaded green roof bag filters (R = 19) operating at low flow rates, the steady-state contribution to the indoor ventilation air is approximately 19 ± 0.5 μg m^{-3} which can be a substantial contribution to the indoor environment given that a typical range of indoor air methanol concentrations is 10 - 30 μg m^{-3} [78].

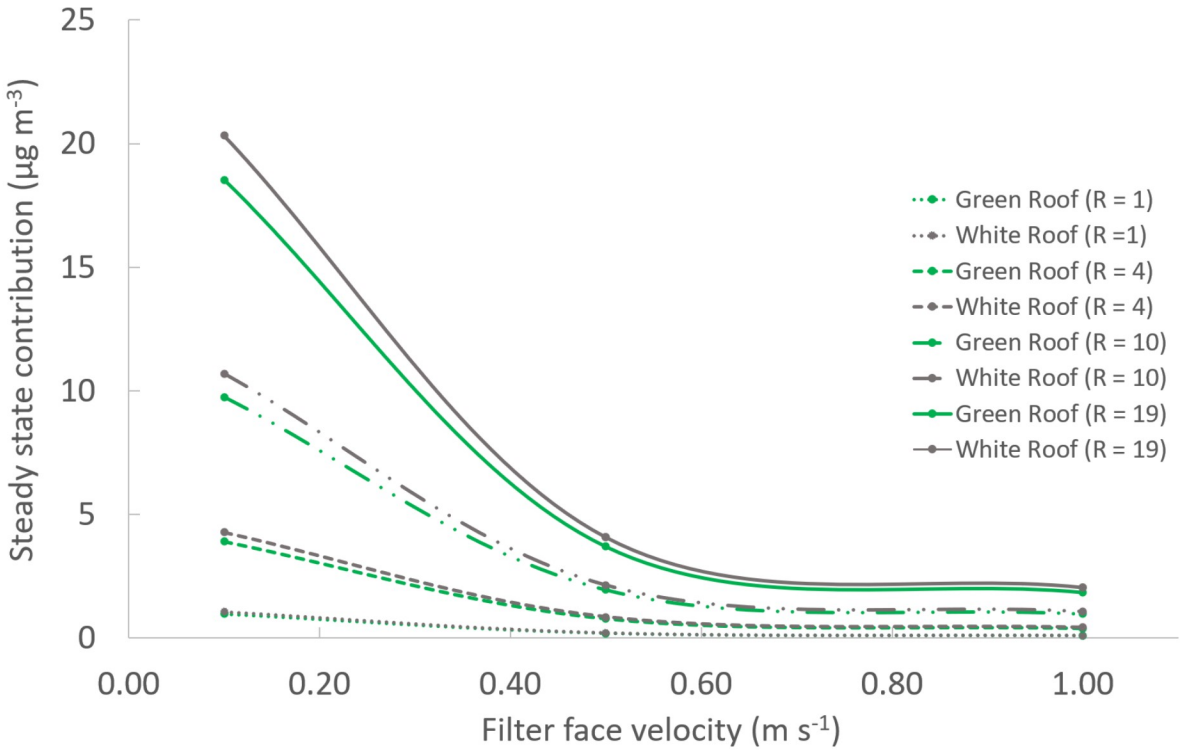

Figure 6. Steady state volatile contribution to the indoor environment for green (GR) and white (WR) roof filters for different filter types; pad filter (R = 1), thick pleated filter (R = 7), and bag filter (R = 19).

For green roof filters from the fall season at 23° C and 50% RH, the measured methanol primary flux was 10.96 ± 3.09 μmol m^{-2} h^{-1} and the respective contribution to the indoor ventilation air is 3.90 ± 0.27, 0.78 ± 0.05, and 0.39 ± 0.03 μg m^{-3} for the low, medium, and high face velocities and pleated filters (R = 4). Similarly, for a fall green roof filter at the same temperature and RH conditions and in the presence of ~180 ppb ozone, the measured flux of formic acid is 3.47 ± 0.78 μmol m^{-2} h^{-1} and the contribution to indoor ventilation air is 1.72 ± 0.38, 0.34 ± 0.08, and 0.17 ± 0.04 μg m^{-3} for pleated filters at low, medium, and

high face velocities, respectively. For thick bag filters (R = 19), the contribution to the ventilation air can be sizeable, 3.48 ± 1.32 μg m^{-3}, relative to measured formic acid concentrations in the indoor environment, approximately 9 μg m^{-3} [79].

4.8. Conclusions

In sum, these results show that contributions of loaded filters to the indoor environment can elevate VOC levels in ventilation air and depend on the filter face velocity and the ratio of filter media to face area. Filter VOC fluxes can vary across seasons and potentially vary due to local rooftop environment. Fluxes of methanol overshadowed the compounds tracked in this study, including in unused filters suggesting high methanol fluxes are intrinsic to some HVAC filters. Variation of VOC fluxes of other selected compounds between filter samples made it difficult to assess trends due to temperature, RH, or seasonal conditions. Green and white roof filters collected different microbial contents in terms of both absolute and relative abundance suggesting roof type may affect the amount and composition of biotic particles depositing on the HVAC filters. No particle formation was observed due to surface ozonolysis across varying temperature, RH, and seasonal conditions. Further studies should quantitively characterize the amount and chemical composition of accumulated mass loaded on the filter. These data would contribute to a more complete understanding of the drivers of emissions and chemistry occurring on loaded HVAC filters that may lead to the gas-phase emissions to indoor ventilation air.

Acknowledgements

This material is based upon work supported by the National Science Foundation under Grant No. 1605843 and 1356679. Any opinions, findings, and conclusions or recommendations expressed in this material are those of the author(s) and do not necessarily reflect the views of the National Science Foundation.

Funding for metagenomic processing, analyses and interpretation were provided by the SCELSE through Singapore Ministry of Education funding grant MOE2013-T3-1-013.

We would like to thank Aurélie Laguerre and Finnegan Clark for their assistance with this project.

5. References

(1) Shafique, M.; Kim, R.; Rafiq, M. Green Roof Benefits, Opportunities and Challenges – A Review. *Renewable and Sustainable Energy Reviews* **2018**, *90*, 757–773. https://doi.org/10.1016/j.rser.2018.04.006.

(2) Sailor, D. J.; Elley, T. B.; Gibson, M. Exploring the Building Energy Impacts of Green Roof Design Decisions – a Modeling Study of Buildings in Four Distinct Climates. *Journal of Building Physics* **2012**, *35* (4), 372–391. https://doi.org/10.1177/1744259111420076.

(3) Clark, C.; Adriaens, P.; Talbot, F. B. Green Roof Valuation: A Probabilistic Economic Analysis of Environmental Benefits. *Environ. Sci. Technol.* **2008**, *42* (6), 2155–2161. https://doi.org/10.1021/es0706652.

(4) Oberndorfer, E.; Lundholm, J.; Bass, B.; Coffman, R. R.; Doshi, H.; Dunnett, N.; Gaffin, S.; Köhler, M.; Liu, K. K. Y.; Rowe, B. Green Roofs as Urban Ecosystems: Ecological Structures, Functions, and Services. *BioScience* **2007**, *57* (10), 823–833. https://doi.org/10.1641/B571005.

(5) Bousselot, J.; Russell, V.; Tolderlund, L.; Celik, S.; Retzlaff, B.; Morgan, S.; Buffam, I.; Coffman, R.; Williams, J.; Mitchell, M. E.; DeSpain, J. Green Roof Research in North America: A Recent History and Future Strategies. 38.

(6) Currie, B. A.; Bass, B. Estimates of Air Pollution Mitigation with Green Plants and Green Roofs Using the UFORE Model. *Urban Ecosyst* **2008**, *11* (4), 409–422. https://doi.org/10.1007/s11252-008-0054-y.

(7) Jeanjean, A. P. R.; Monks, P. S.; Leigh, R. J. Modelling the Effectiveness of Urban Trees and Grass on PM2.5 Reduction via Dispersion and Deposition at a City Scale. *Atmospheric Environment* **2016**, *147*, 1–10. https://doi.org/10.1016/j.atmosenv.2016.09.033.

(8) Ramasubramanian, P.; Starry, O.; Rosenstiel, T.; Gall, E. T. Pilot Study on the Impact of Green Roofs on Ozone Levels near Building Ventilation Air Supply. *Building and Environment* **2019**, *151*, 43–53. https://doi.org/10.1016/j.buildenv.2019.01.023.

(9) Xing, Y.; Brimblecombe, P. Role of Vegetation in Deposition and Dispersion of Air Pollution in Urban Parks. *Atmospheric Environment* **2019**, *201*, 73–83. https://doi.org/10.1016/j.atmosenv.2018.12.027.

(10) Abbass, O. A.; Sailor, D. J.; Gall, E. T. Ozone Removal Efficiency and Surface Analysis of Green and White Roof HVAC Filters. *Building and Environment* **2018**, *136*, 118–127. https://doi.org/10.1016/j.buildenv.2018.03.042.

(11) Batterman, S. A.; Burge, H. HVAC Systems As Emission Sources Affecting Indoor Air Quality: A Critical Review. *HVAC&R Research* **1995**, *1* (1), 61–78. https://doi.org/10.1080/10789669.1995.10391309.

(12) Bernstein, R. S.; Sorenson, W. G.; Garabrant, D.; Reaux, C.; Treitman, R. D. Exposures to Respirable, AirbornePenicillium from a Contaminated Ventilation System: Clinical, Environmental and Epidemiological Aspects. *American Industrial Hygiene Association Journal* **1983**, *44* (3), 161–169. https://doi.org/10.1080/15298668391404581.

(13) Tang, W.; Kuehn, T. H.; Simcik, M. F. Effects of Temperature, Humidity and Air Flow on Fungal Growth Rate on Loaded Ventilation Filters. *Journal of Occupational and Environmental Hygiene* **2015**, *12* (8), 525–537. https://doi.org/10.1080/15459624.2015.1019076.

(14) Ahearn, D. G. Fungal Colonization of Air Filters and Insulation in a Multi-Story Office Building: Production of Volatile Organics. *Current Microbiology* **1997**, *35* (5), 305–308. https://doi.org/10.1007/s002849900259.

(15) Weschler, C. J. Indoor/Outdoor Connections Exemplified by Processes That Depend on an Organic Compound's Saturation Vapor Pressure. *Atmospheric Environment* **2003**, *37* (39–40), 5455–5465. https://doi.org/10.1016/j.atmosenv.2003.09.022.

(16) Hyttinen, M.; Pasanen, P.; Kalliokoski, P. Adsorption and Desorption of Selected VOCs in Dust Collected on Air Filters. *Atmospheric Environment* **2001**, *35* (33), 5709–5716. https://doi.org/10.1016/S1352-2310(01)00376-4.
(17) Hyttinen, M.; Pasanen, P.; Björkroth, M.; Kalliokoski, P. Odors and Volatile Organic Compounds Released from Ventilation Filters. *Atmospheric Environment* **2007**, *41* (19), 4029–4039. https://doi.org/10.1016/j.atmosenv.2007.01.029.
(18) Schleibinger, H.; Ruden, H. Air Filters from HVAC Systems as Possible Source of Volatile Organic Compounds (VOC) - Laboratory and Field Assays. *Atmospheric Environment* **1999**, 7.
(19) Bekö, G.; Clausen, G.; Weschler, C. J. Further Studies of Oxidation Processes on Filter Surfaces: Evidence for Oxidation Products and the Influence of Time in Service. *Atmospheric Environment* **2007**, *41* (25), 5202–5212. https://doi.org/10.1016/j.atmosenv.2006.07.063.
(20) Beko, G.; Halas, O.; Clausen, G.; Weschler, C. J. Initial Studies of Oxidation Processes on Filter Surfaces and Their Impact on Perceived Air Quality. *Indoor Air* **2006**, *16* (1), 56–64. https://doi.org/10.1111/j.1600-0668.2005.00401.x.
(21) Zhao, P.; Siegel, J. A.; Corsi, R. L. Ozone Removal by HVAC Filters. *Atmospheric Environment* **2007**, *41* (15), 3151–3160. https://doi.org/10.1016/j.atmosenv.2006.06.059.
(22) Hyttinen, M.; Pasanen, P.; Kalliokoski, P. Removal of Ozone on Clean, Dusty and Sooty Supply Air Filters. *Atmospheric Environment* **2006**, *40* (2), 315–325. https://doi.org/10.1016/j.atmosenv.2005.09.040.
(23) Zhao, P.; Siegel, J.; Corsi, R. Ozone Removal by Residential HVAC Filters. *Indoor Air* **2005**, 5.
(24) Lin, C.-C.; Chen, H.-Y. Impact of HVAC Filter on Indoor Air Quality in Terms of Ozone Removal and Carbonyls Generation. *Atmospheric Environment* **2014**, *89*, 29–34. https://doi.org/10.1016/j.atmosenv.2014.02.020.
(25) Destaillats, H.; Chen, W.; Apte, M. G.; Li, N.; Spears, M.; Almosni, J.; Brunner, G.; Zhang, J. (Jensen); Fisk, W. J. Secondary Pollutants from Ozone Reactions with Ventilation Filters and Degradation of Filter Media Additives. *Atmospheric Environment* **2011**, *45* (21), 3561–3568. https://doi.org/10.1016/j.atmosenv.2011.03.066.
(26) Sidheswaran, M.; Chen, W.; Miller, R.; Cohn, S.; Kumagai, K.; Destaillats, H. Formaldehyde Emissions from Ventilation Filter Under Different Relative Humidity Conditions. **2013**, 27.
(27) Evans, R. C.; Tingey, D. T.; Gumpertz, M. L.; Burns, W. F. Estimates of Isoprene and Monoterpene Emission Rates in Plants. *Botanical Gazette* **1982**, *143* (3), 304–310. https://doi.org/10.1086/botanicalgazette.143.3.2474826.
(28) Singh, B.; Sharma, R. A. Plant Terpenes: Defense Responses, Phylogenetic Analysis, Regulation and Clinical Applications. *3 Biotech* **2015**, *5* (2), 129–151. https://doi.org/10.1007/s13205-014-0220-2.
(29) Wang, C.; Waring, M. S. Secondary Organic Aerosol Formation Initiated from Reactions between Ozone and Surface-Sorbed Squalene. *Atmospheric Environment* **2014**, *84*, 222–229. https://doi.org/10.1016/j.atmosenv.2013.11.009.
(30) Waring, M. S.; Siegel, J. A. Indoor Secondary Organic Aerosol Formation Initiated from Reactions between Ozone and Surface-Sorbed D -Limonene. *Environ. Sci. Technol.* **2013**, *47* (12), 6341–6348. https://doi.org/10.1021/es400846d.
(31) Carslaw, N.; Ashmore, M.; Terry, A. C.; Carslaw, D. C. Crucial Role for Outdoor Chemistry in Ultrafine Particle Formation in Modern Office Buildings. *Environ. Sci. Technol.* **2015**, 8.
(32) Luhung, I.; Wu, Y.; Ng, C. K.; Miller, D.; Cao, B.; Chang, V. W.-C. Protocol Improvements for Low Concentration DNA-Based Bioaerosol Sampling and Analysis. *PLOS ONE* **2015**, 18.
(33) Martin, M. Cutadapt Removes Adapter Sequences from High-Throughput Sequencing Reads. 3.
(34) Menzel, P. Fast and Sensitive Taxonomic Classification for Metagenomics with Kaiju. *NATURE COMMUNICATIONS* 10.

(35) Huson, D. H.; Auch, A. F.; Qi, J.; Schuster, S. C. MEGAN Analysis of Metagenomic Data. 11.
(36) Destaillats, H. Secondary Pollutants from Ozone Reactions with Ventilation Filters and Degradation of Filter Media Additives. *Atmospheric Environment* **2011**, 8.
(37) Potard, K.; Monard, C.; Le Garrec, J.-L.; Caudal, J.-P.; Le Bris, N.; Binet, F. Organic Amendment Practices as Possible Drivers of Biogenic Volatile Organic Compounds Emitted by Soils in Agrosystems. *Agriculture, Ecosystems & Environment* **2017**, *250*, 25–36. https://doi.org/10.1016/j.agee.2017.09.007.
(38) Maleknia, S. D.; Bell, T. L.; Adams, M. A. PTR-MS Analysis of Reference and Plant-Emitted Volatile Organic Compounds. *International Journal of Mass Spectrometry* **2007**, *262* (3), 203–210. https://doi.org/10.1016/j.ijms.2006.11.010.
(39) Abis, L.; Loubet, B.; Ciuraru, R.; Lafouge, F.; Dequiedt, S.; Houot, S.; Maron, P. A.; Bourgeteau-Sadet, S. Profiles of Volatile Organic Compound Emissions from Soils Amended with Organic Waste Products. *Science of The Total Environment* **2018**, *636*, 1333–1343. https://doi.org/10.1016/j.scitotenv.2018.04.232.
(40) Nemecek-Marshall, M.; MacDonald, R. C.; Franzen, J. J.; Wojciechowski, C. L.; Fall, R. Methanol Emission from Leaves (Enzymatic Detection of Gas-Phase Methanol and Relation of Methanol Fluxes to Stomatal Conductance and Leaf Development). *Plant Physiol.* **1995**, *108* (4), 1359–1368. https://doi.org/10.1104/pp.108.4.1359.
(41) Greenberg, J. P.; Asensio, D.; Turnipseed, A.; Guenther, A. B.; Karl, T.; Gochis, D. Contribution of Leaf and Needle Litter to Whole Ecosystem BVOC Fluxes. *Atmospheric Environment* **2012**, 10.
(42) Kim, S.; Karl, T.; Guenther, A.; Tyndall, G.; Orlando, J.; Harley, P.; Rasmussen, R.; Apel, E. Emissions and Ambient Distributions of Biogenic Volatile Organic Compounds (BVOC) in a Ponderosa Pine Ecosystem: Interpretation of PTR-MS Mass Spectra. *Atmos. Chem. Phys.* **2010**, *10* (4), 1759–1771. https://doi.org/10.5194/acp-10-1759-2010.
(43) Laothawornkitkul, J.; Taylor, J. E.; Paul, N. D.; Hewitt, C. N. Biogenic Volatile Organic Compounds in the Earth System. *New Phytologist* **2009**, *183* (1), 27–51. https://doi.org/10.1111/j.1469-8137.2009.02859.x.
(44) Bourtsoukidis, E.; Bonn, B.; Noe, S. M. On-Line Field Measurements of BVOC Emissions from Norway Spruce (Picea Abies) at the Hemiboreal SMEAR-Estonia Site under Autumn Conditions. *19*, 15.
(45) Bamberger, I.; Hörtnagl, L.; Schnitzhofer, R.; Graus, M.; Ruuskanen, T. M.; Müller, M.; Dunkl, J.; Wohlfahrt, G.; Hansel, A. BVOC Fluxes above Mountain Grassland. *Biogeosciences* **2010**, *7* (5), 1413–1424. https://doi.org/10.5194/bg-7-1413-2010.
(46) Sanhueza, E.; Andreae, M. O. Emission of Formic and Acetic Acids from Tropical Savanna Soils. *Geophys. Res. Lett.* **1991**, *18* (9), 1707–1710. https://doi.org/10.1029/91GL01565.
(47) Coleman, B. K.; Destaillats, H.; Hodgson, A. T.; Nazaroff, W. W. Ozone Consumption and Volatile Byproduct Formation from Surface Reactions with Aircraft Cabin Materials and Clothing Fabrics. *Atmospheric Environment* **2008**, *42* (4), 642–654. https://doi.org/10.1016/j.atmosenv.2007.10.001.
(48) Friedman, M. The Use of Ranks to Avoid the Assumption of Normality Implicit in the Analysis of Variance. *null* **1937**, *32* (200), 675–701. https://doi.org/10.1080/01621459.1937.10503522.
(49) Gabdrashova, R.; Nurzhan, S.; Naseri, M.; Bekezhankyzy, Z.; Gimnkhan, A.; Malekipirbazari, M.; Tabesh, M.; Khanbabaie, R.; Crape, B.; Buonanno, G.; Hopke, P. K.; Amouei Torkmahalleh, A.; Amouei Torkmahalleh, M. The Impact on Heart Rate and Blood Pressure Following Exposure to Ultrafine Particles from Cooking Using an Electric Stove. *Science of The Total Environment* **2021**, *750*, 141334. https://doi.org/10.1016/j.scitotenv.2020.141334.
(50) Cosgrove, D. J. Growth of the Plant Cell Wall. *Nat Rev Mol Cell Biol* **2005**, *6* (11), 850–861. https://doi.org/10.1038/nrm1746.

(51) Mellerowicz, E.; Sundberg, B. Wood Cell Walls: Biosynthesis, Developmental Dynamics and Their Implications for Wood Properties. *Current Opinion in Plant Biology* **2008**, *11* (3), 293–300. https://doi.org/10.1016/j.pbi.2008.03.003.

(52) Risholm-Sundman, M.; Lundgren, M.; Vestin, E.; Herder, P. Emissions of Acetic Acid and Other Volatile Organic Compounds from Different Species of Solid Wood. *Holz als Roh-und Werkstoff* **1998**, *56* (2), 125–129. https://doi.org/10.1007/s001070050282.

(53) Gray, C. M.; Monson, R. K.; Fierer, N. Emissions of Volatile Organic Compounds during the Decomposition of Plant Litter. *J. Geophys. Res.* **2010**, *115* (G3), G03015. https://doi.org/10.1029/2010JG001291.

(54) Warneke, C.; Karl, T.; Judmaier, H.; Hansel, A.; Jordan, A.; Lindinger, W.; Crutzen, P. J. Acetone, Methanol, and Other Partially Oxidized Volatile Organic Emissions from Dead Plant Matter by Abiological Processes: Significance for Atmospheric HO_x Chemistry. *Global Biogeochem. Cycles* **1999**, *13* (1), 9–17. https://doi.org/10.1029/98GB02428.

(55) Rantala, P.; Järvi, L.; Taipale, R.; Laurila, T. K.; Patokoski, J.; Kajos, M. K.; Kurppa, M.; Haapanala, S.; Siivola, E.; Petäjä, T.; Ruuskanen, T. M.; Rinne, J. Anthropogenic and Biogenic Influence on VOC Fluxes at an Urban Background Site in Helsinki, Finland. *Atmos. Chem. Phys.* **2016**, *16* (12), 7981–8007. https://doi.org/10.5194/acp-16-7981-2016.

(56) Lange, B. M.; Ahkami, A. Metabolic Engineering of Plant Monoterpenes, Sesquiterpenes and Diterpenes-Current Status and Future Opportunities. *Plant Biotechnol J* **2013**, *11* (2), 169–196. https://doi.org/10.1111/pbi.12022.

(57) Sharkey, T. D.; Yeh, S. Isoprene Emission from Plants. *Annu. Rev. Plant. Physiol. Plant. Mol. Biol.* **2001**, *52* (1), 407–436. https://doi.org/10.1146/annurev.arplant.52.1.407.

(58) Wang, C.; Collins, D. B.; Arata, C.; Goldstein, A. H.; Mattila, J. M.; Farmer, D. K.; Ampollini, L.; DeCarlo, P. F.; Novoselac, A.; Vance, M. E.; Nazaroff, W. W.; Abbatt, J. P. D. Surface Reservoirs Dominate Dynamic Gas-Surface Partitioning of Many Indoor Air Constituents. *Sci. Adv.* **2020**, *6* (8), eaay8973. https://doi.org/10.1126/sciadv.aay8973.

(59) Thanomsub, B.; Anupunpisit, V.; Chanphetch, S.; Watcharachaipong, T.; Poonkhum, R.; Srisukonth, C. Effects of Ozone Treatment on Cell Growth and Ultrastructural Changes in Bacteria. *J. Gen. Appl. Microbiol.* **2002**, *48* (4), 193–199. https://doi.org/10.2323/jgam.48.193.

(60) Guzel-Seydim, Z. B.; Greene, A. K.; Seydim, A. C. Use of Ozone in the Food Industry. *LWT - Food Science and Technology* **2004**, *37* (4), 453–460. https://doi.org/10.1016/j.lwt.2003.10.014.

(61) Schulz, S.; Dickschat, J. S. Bacterial Volatiles: The Smell of Small Organisms. *Nat. Prod. Rep.* **2007**, *24* (4), 814. https://doi.org/10.1039/b507392h.

(62) Li, M.; Nian, R.; Xian, M.; Zhang, H. Metabolic Engineering for the Production of Isoprene and Isopentenol by Escherichia Coli. *Appl Microbiol Biotechnol* **2018**, *102* (18), 7725–7738. https://doi.org/10.1007/s00253-018-9200-5.

(63) Sethia, P.; Ahuja, M.; Rangaswamy, V. Metabolic Engineering of Microorganisms to Produce Isoprene. *11* (419), 9.

(64) Schnitzler, J.-P.; Louis, S.; Behnke, K.; Loivamäki, M. Poplar Volatiles - Biosynthesis, Regulation and (Eco)Physiology of Isoprene and Stress-Induced Isoprenoids: Plant Volatiles of Poplar. *Plant Biology* **2009**, *12* (2), 302–316. https://doi.org/10.1111/j.1438-8677.2009.00284.x.

(65) Vickers, C. E.; Possell, M.; Cojocariu, C. I.; Velikova, V. B.; Laothawornkitkul, J.; Ryan, A.; Mullineaux, P. M.; Nicholas Hewitt, C. Isoprene Synthesis Protects Transgenic Tobacco Plants from Oxidative Stress. *Plant, Cell & Environment* **2009**, *32* (5), 520–531. https://doi.org/10.1111/j.1365-3040.2009.01946.x.

(66) Velikova, V.; Fares, S.; Loreto, F. Isoprene and Nitric Oxide Reduce Damages in Leaves Exposed to Oxidative Stress. *Plant, Cell & Environment* **2008**, *31* (12), 1882–1894. https://doi.org/10.1111/j.1365-3040.2008.01893.x.

(67) Vaida Valuntait; Šerevicien, V.; Girgždien, D.; Paliulis. Relative Humidity and Temperature Impact to Ozone And Nitrogen Oxides Removal Rate in The Experimental Chamber. *Journal of Environmental Engineering and Landscape Management*.
(68) Hoch, J. M. K.; Rhodes, M. E.; Shek, K. L.; Dinwiddie, D.; Hiebert, T. C.; Gill, A. S.; Salazar Estrada, A. E.; Griffin, K. L.; Palmer, M. I.; McGuire, K. L. Soil Microbial Assemblages Are Linked to Plant Community Composition and Contribute to Ecosystem Services on Urban Green Roofs. *Frontiers in Ecology and Evolution* **2019**, *7*, 198. https://doi.org/10.3389/fevo.2019.00198.
(69) Anderson, M.; Lambrinos, J.; Schroll, E. The Potential Value of Mosses for Stormwater Management in Urban Environments. *Urban Ecosystems* **2010**, *13*, 319–332.
(70) Ander, P.; Eriksson, K.-E. Methanol Formation during Lignin Degradation by Phanerochaete Chrysosporium. *Applied Microbiology and Biotechnology* **1985**, *21* (1), 96–102. https://doi.org/10.1007/BF00252369.
(71) Zhang, Junfeng.; Wilson, W. E.; Lioy, P. J. Indoor Air Chemistry: Formation of Organic Acids and Aldehydes. *Environ. Sci. Technol.* **1994**, *28* (11), 1975–1982. https://doi.org/10.1021/es00060a031.
(72) Glasius, M.; Lahaniati, M.; Calogirou, A.; Di Bella, D.; Jensen, N. R.; Hjorth, J.; Kotzias, D.; Larsen, B. R. Carboxylic Acids in Secondary Aerosols from Oxidation of Cyclic Monoterpenes by Ozone. *Environ. Sci. Technol.* **2000**, *34* (6), 1001–1010. https://doi.org/10.1021/es990445r.
(73) Morrison, G. C.; Nazaroff, W. W. Ozone Interactions with Carpet: Secondary Emissions of Aldehydes. *Environ. Sci. Technol.* **2002**, *36* (10), 2185–2192. https://doi.org/10.1021/es0113089.
(74) Nawrocki, J.; Świetlik, J.; Raczyk-Stanisławiak, U.; Dąbrowska, A.; Biłozor, S.; Ilecki, W. Influence of Ozonation Conditions on Aldehyde and Carboxylic Acid Formation. *Ozone: Science & Engineering* **2003**, *25* (1), 53–62. https://doi.org/10.1080/713610650.
(75) US Environmental Protection Agency. Health Assessment Document for Acetaldehyde. **1987**.
(76) Thompson, M. Administered by Inhalation to F344/N Rats and B6C3F1 Mice. *Toxicity Report Series* No. 19, 62. **1992**.
(77) Bergmans, L.; Moisiadis, P.; Van Meerbeek, B.; Quirynen, M.; Lambrechts, P. Microscopic Observation of Bacteria: Review Highlighting the Use of Environmental SEM. *Int Endod J* **2005**, *38* (11), 775–788. https://doi.org/10.1111/j.1365-2591.2005.00999.x.
(78) Solomon, S. J.; Schade, G. W.; Kuttippurath, J.; Ladstätter-Weissenmayer, A.; Burrows, J. P. VOC Concentrations in an Indoor Workplace Environment of a University Building. *Indoor and Built Environment* **2008**, *17* (3), 260–268. https://doi.org/10.1177/1420326X08090822.
(79) Zhang, J.; Wilson, W.; Lioy, P. Sources of Organic Acids in Indoor Air: A Field Study. *Journal of exposure analysis and environmental epidemiology* **1994**, *4* (1), 25—47.